

# Curious Variables Experiment (CURVE). Three Periodicities of BF Ara\*

A. Olech<sup>1</sup>, A. Rutkowski<sup>1</sup>, and A. Schwarzenberg-Czerny<sup>1,2</sup>

<sup>1</sup> Nicolaus Copernicus Astronomical Center, Polish Academy of Sciences, ul. Bartycka 18,  
00-716 Warszawa, Poland,  
e-mail: (olech,rudy,alex)@camk.edu.pl

<sup>2</sup> A. Mickiewicz University Observatory, ul. Słoneczna 36, 60-286 Poznań, Poland.

## Abstract

We report CCD photometry of the dwarf nova BF Ara throughout fifteen consecutive nights in quiescence. Light curve in this interval is dominated by a large amplitude ( $\sim 0.8$  mag) modulation consisting two periods. Higher amplitude signal is characterized by period of 0.082159(4) days, which was increasing at the rate of  $\dot{P}/P_{\text{sh}} = 3.8(3) \cdot 10^{-5}$ . Weaker and stable signal has period of 0.084176(21) days. Knowing the superhump period of BF Ara determined by Kato et al. (2003) and equal to 0.08797(1) days, the first modulation is interpreted as quiescent negative superhump arising from retrograde precession of tilted accretion disk and the latter one as an orbital period of the binary. The respective period excess and defect are  $\epsilon_+ = 4.51\% \pm 0.03\%$  and  $\epsilon_- = -2.44\% \pm 0.02\%$ . Thus BF Ara is yet another in-the-gap nova with mass ratio of around  $q \approx 0.21$ .

**Key words:** Stars: individual: BF Ara – binaries: close – novae, cataclysmic variables

## 1 Introduction

The SU UMa variables are a subclass of dwarf novae characterized by the presence of two types of eruptions - normal outburst having an amplitude of 2-3 mag and repeating typically every few tens of days and superoutbursts with amplitude of 3-4 mag, lasting few times longer and occurring every year or so.

These stars are believed to be binary systems consisting of the white dwarf primary and low mass main-sequence secondary filling its Roche lobe and losing material which forms an accretion disc around the primary. Almost all SU UMa stars are close binaries with orbital period from 1.25 to slightly over 2 hours.

This behaviour is now quite well understood within the frame of the thermal-tidal instability model (see Osaki 1996 for review). Normal outbursts are caused by the thermal instability connected with transition of the material in the disc from neutral to ionized state. Superoutbursts are a result of combined thermal and tidal instability, which, working together, are very effective with sweeping out the matter from the disc.

During the superoutburst, the characteristic tooth-shape light modulations with a period a few percent longer than the orbital period of the binary are observed. They are most probably the result of accretion disc "precession" (in fact it is not classical precession but change of the position of the line of apsides) caused by gravitational perturbations from the secondary. These perturbations are most effective when disc particles moving in eccentric orbits enter the 3:1 resonance. Then the superhump period is simply the beat period between orbital and "precession" rate periods.

---

\*Based on observations at SAAO

At the beginning of the 1990s, the quite simple class of SU UMas started to be more complicated. The systems showing superhumps were divided into four subgroups:

- WZ Sge stars, characterized by an extremely long quiescent state, going into superoutburst every  $\sim 10$  years and showing no or very infrequent ordinary outbursts (Patterson et al. 2002),
- ordinary SU UMa stars,
- ER UMa stars - systems characterized by an extremely short supercycle (20-60 days), a short interval between normal outbursts (3-4 days) and small amplitude (2–3 mag) of superoutbursts (Kato and Kunjaya 1995, Robertson et al. 1995),
- permanent superhumpers - high accretion rate systems being permanently in superoutbursts (Skillman and Patterson 1993).

We now believe that the classes listed above represent increasing mass transfer. Systems with mass transfer rates as low as  $10^{15}$  g/s are inactive, quiet and evolved stars of WZ Sge type containing brown dwarf degenerated secondary. Classical SU UMa stars have mass transfer rates one magnitude higher and go into the superoutburst every year or so. ER UMa stars are high mass transfer rate systems (few times per  $10^{16}$  g/s) showing frequent and relatively long superoutburst lasting for about half of the supercycle. The explanation of the shortest supercycles involves poorly understood mechanisms causing premature quench of the eruption (Osaki 1995). And finally, permanent superhumpers are system with accretion disc which is thermally stable and tidally unstable all the time, i.e. being in permanent state of superoutburst.

## 2 Observations and data reduction

In order to firmly establish the mutual relations between these SU UMa subclasses one has to study systems located near to the borders between them. For these purposes we selected several poorly studied objects which are very interesting from the point of view of the theory which describes the origin of superhumps in dwarf novae systems. For a report of our northern hemisphere work performed at the Ostrowik observatory see previous reports on our CURVE project, e.g. Rutkowski et al. (2007). Since a significant number of these systems is located in the southern hemisphere, we applied for the observation time in South African Astronomical Observatory (SAAO). For a pilot study we had been allocated time from August 15 to September 11 on Elizabeth telescope at SAAO.

The observations were performed by one of us (A.R.) using a 1-m Cassegrain telescope of 8.5-m focal length. The telescope worked with CCD camera "STE3", back illuminated chip manufactured by SITE of size  $512 \times 512$  pixels. The image scale was 0.31 arcsec/pix providing a  $158 \times 158$  arcsec field of view. The camera worked with liquid nitrogen cooling. Technology of the whole system allows to minimize the influence of noises like bias and dark current. Thanks to that it was not necessary to obtain the bias and dark frames. The filters wheel was equipped with Johnson-Cousins *UBV(RI)* filters but most of observations were obtained in white light as we wanted to examine temporal behaviour of light curve and have good quality photometry of faint objects. We were using exposure times ranging from 100 to 200 sec, depending on weather conditions and actual brightness of the object. Data reduction was performed using a standard procedure based on IRAF package.<sup>1</sup> The profile photometry has been derived using the DAOPHOTII package (Stetson 1987). The differential photometry provided measurements with accuracy in most cases around or below 0.01 mag.

---

<sup>1</sup> IRAF is distributed by the National Optical Astronomy Observatory, which is operated by the Association of Universities for Research in Astronomy, Inc., under cooperative agreement with the National Science Foundation.

### 3 BF Ara

One object from our southern sky survey is dwarf nova BF Ara. It was discovered as a variable by Shapley and Swope (1934) but the nature of its light variations remained unknown until work of Bruch (1983) who made *U*, *B* and *V* photometry of this object during one night in its bright state. The light curve exhibited a tooth-shape hump with an amplitude of 0.25 mag and period of roughly two hours. The conclusion was that BF Ara might belong to the SU UMa dwarf novae.

In the years 1997–2001 BF Ara was regularly monitored by VSNET Collaborators. These data allowed Kato et al. (2001) to find that BF Ara is one of the most active normal SU UMa stars with mean interval between the successive superoutbursts amounting to 83.4 days. Except for ER UMa stars, it was the shortest supercycle ever recorded, leaving SS UMi with its 84.7 day value behind (however, as was demonstrated by Olech et al. 2006, SS UMi could sometimes switch to normal behavior with much longer supercycles).

Detailed CCD photometry of BF Ara in superoutburst was done by Kato et al. (2003) in August 2002. Good coverage of the eruption allowed for precise determination of the superhump period which was 0.08797(1) days and seemed to be constant throughout the entire superoutburst. Other characteristics of the star showed that it resembles ordinary SU UMa stars rather than active ER UMa objects.

Table 1 presents the journal of our CCD observations of BF Ara. In total, we observed the star for almost 31 hours on 15 nights and collected 666 exposures.

Table 1: Observational journal for the BF Ara campaign.

Date in 2007	Start [UT]	End [UT]	No. of points	Duration [h]
Aug 27	54339.71157	54339.80641	59	2.28
Aug 28	54340.71024	54340.79588	53	2.06
Aug 29	54341.70433	54341.80002	60	3.00
Aug 30	54342.74061	54342.80826	43	1.62
Aug 31	54343.70650	54343.79958	59	2.23
Sep 01	54344.70766	54344.77470	39	1.61
Sep 02	54345.70788	54345.79830	56	2.17
Sep 03	54346.70939	54346.79243	52	1.99
Sep 04	54347.71067	54347.79506	44	2.03
Sep 05	54348.71216	54348.79240	45	1.93
Sep 06	54349.71031	54349.79907	28	2.13
Sep 07	54350.71358	54350.79352	30	1.91
Sep 08	54351.71438	54351.79802	33	2.01
Sep 09	54352.71238	54352.79422	32	1.96
Sep 10	54353.71619	54353.79464	33	1.88

### 4 Light curve

The light curve of BF Ara from 15 consecutive nights starting on Aug 27 and ending on Sep 10, 2007 is presented in Fig. 1. Such a span corresponds to the Rayleigh frequency resolution of 0.07 c/d. The median separation of observations is 0.0016 d and thus the effective Nyquist frequency amounts to 300 c/d. Time sampling of our observations is non optimal. Large daily gaps and short nightly runs produced a spectral window with 10 aliases separated by 1 c/d exceeding half power of the central peak. In consequence any period estimated from our data may suffer from the 1 c/d ambiguity. In order to suppress any low frequency long-term

irregular variations night averages were subtracted from the observed magnitudes.

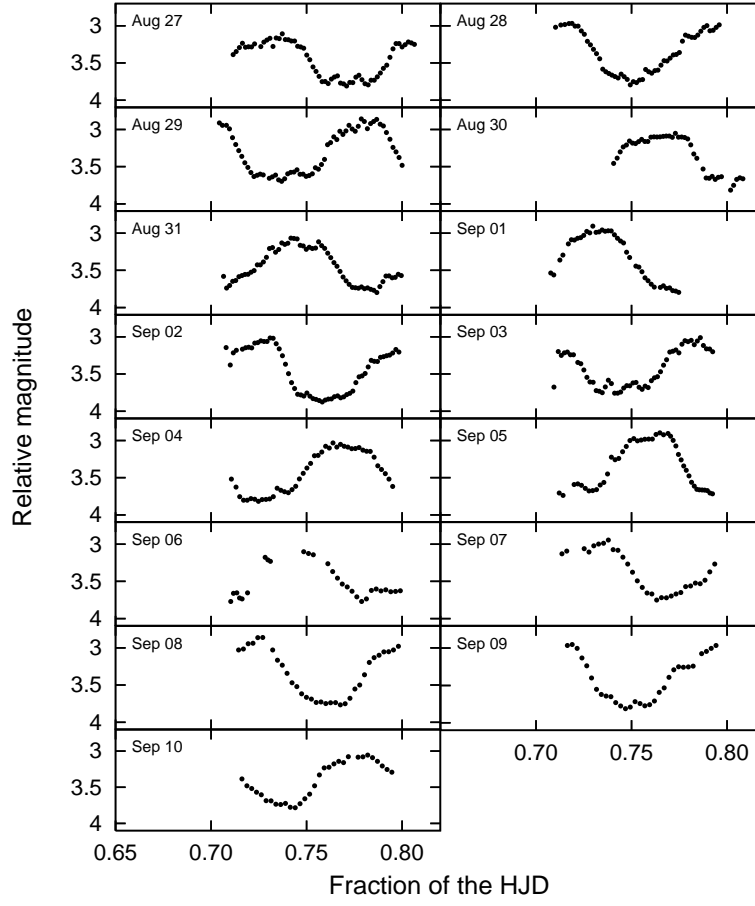


Figure 1: Light curves of BF Ara obtained on 15 consecutive nights of August and September of 2007.

#### 4.1 A permanent hump

Presence of a periodic modulation with peak-to-peak amplitude reaching up to 1 magnitude was apparent from first glance at the data. The harmonic analysis-of-variance (ANOVA - Schwarzenberg-Czerny, 1996) periodogram revealed a pronounced alias pattern centered at the frequency  $f_0 \approx 12.173$  c/d (Fig. 2).

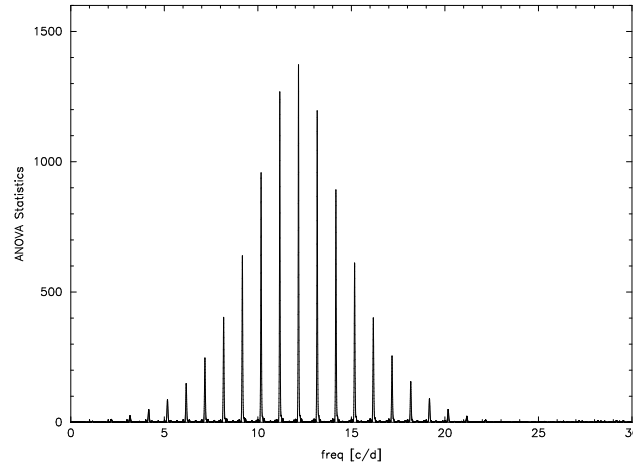


Figure 2: The harmonic analysis-of-variance (ANOVA) periodogram for light curves of BF Ara.

However, both frequency and amplitude did vary during our observations. This became first apparent after splitting data in two halves and analysing them separately. Fitting by least squares of Fourier series of 3 harmonics yields frequencies 12.2013 and 12.1602 c/d for the early and late observations, respectively. The corresponding amplitudes of first harmonics are 0.79 and 0.68 mag.

In order to study the change of frequency in more detail we assumed linear dependence of the fundamental frequency and fitted all data with a Fourier series of 3 harmonics. The best fit yields  $f_0 = 12.1765 \pm 0.0011$  c/d and  $df_0/dt = -0.00529 \text{ c/d}^2$ , i.e.  $P = 0.082125$  d and  $dP/dt = 3.57 \cdot 10^{-5}$ . These values correspond to the mean epoch of 2454345.8583 HJD. Our errors account for correlation of 3.2 residuals, on the average (Schwarzenberg-Czerny, 1991). In our fit the  $2f_0$  and  $3f_0$  harmonics are significant, as they exceed errors 3 times or more. In Fig. 2 we refrained from plotting of the AOV periodogram for 3 harmonics, as it esthetic is diminished by ghost sub-harmonics  $f_0/2$  and  $f_0/3$ . However, its closer inspection reveals that because of extra information from harmonics, its  $\pm 1$  c/d aliases are damped compared to Fig. 2. The combined evidence makes us to believe that for the  $f_0$  frequency the 1 c/d ambiguity remains insignificant. Accounting for the frequency change improved our fit significantly. The corresponding F statistics rose from 1376 to 2213. The corresponding shift of phase at time limits of our observations reaches as much as 0.17 of the period.

## 4.2 Secondary modulation

Prewhitening our data with a constant frequency  $f_0$  yields an unsatisfactory result. Several overlapping alias patterns remain in the residual periodogram. However, subtraction of the Fourier series accounting for period change performed well. The periodogram of residuals becomes clean except for a single alias pattern centered at  $f = 12.88$  c/d (Fig. 3). Note that several alias peaks of comparable height reach values as high as 100. For a statistician the following conclusion holds: i) the periodic modulation is detected securely and ii) no unique value of frequency  $f$  may be assigned. No contradiction exists between i) and ii) as in statistics they correspond to very different procedures: hypotheses testing and parameter estimation. To be conservative, we ought to account here for correlation of 2.4 points on the average (Schwarzenberg-Czerny, 1991). Still, detection in i) remains significant well above the confidence level of 0.999. As far as ii) is concerned, the modulation discussed in this section corresponds to the signal-to-noise as small as  $S/N = 1$  and power in harmonics remains negligible, unlike in Sect. 4.1. In such a situation and for our poor window function the power in  $\pm 1$  c/d aliases almost reaches that of the central peak, making our frequency determination ambiguous.

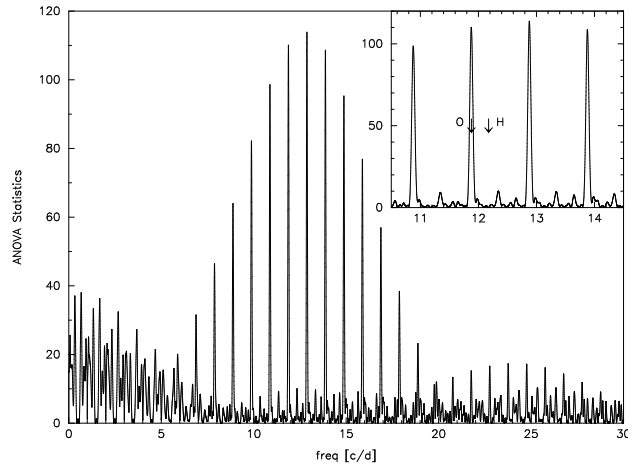


Figure 3: The harmonic analysis-of-variance (ANOVA) periodogram for prewhitened light curves of BF Ara. Inset shows close-up of the frequency pattern in the vicinity of main peak. The arrows marked *O* and *H* indicate respectively the superhump and orbital frequencies

At this point we use the extra information from previous observations of superhumps in BF Ara (Kato et al. 2003) and identify  $f_1 = 11.8799 \pm 0.0030$  c/d as the true frequency of the modulation. Its nature will be discussed later. The corresponding (half)amplitude is  $0.072 \pm 0.010$  mag. Subtraction of this latter sinusoid leaves no significant features in the periodogram up to its effective Nyquist frequency of 300 c/d.

## 5 The O-C diagram

As we already mentioned, higher amplitude signal was changing its frequency with time. To check its behaviour we decided to use the  $O - C$  analysis for times of maxima and minima. They were determined by fitting the polynomials to the observational points in the vicinity of their extrema. We were able to determine 15 times of maxima and 13 times of minima, which are listed in Table 2 together with associated errors, cycle numbers  $E$ , and  $O - C$  values.

Table 2: Times of maxima and minima observed in the light curve of BF Ara in quiescence.

Cycle $E$	HJD <sub>max</sub> - 2454300 [d]	Error [d]	$O - C$ [cycles]	Cycle $E$	HJD <sub>min</sub> - 2454300 [d]	Error [d]	$O - C$ [cycles]
0	39.7340	0.001	0.037	0	39.7710	0.001	0.086
12	40.7189	0.001	0.024	12	40.7495	0.004	-0.008
25	41.7860	0.002	0.011	24	41.7370	0.002	0.007
37	42.7690	0.001	-0.025	37	42.8020	0.002	-0.035
49	43.7563	0.001	-0.009	49	43.7868	0.001	-0.052
61	44.7380	0.002	-0.061	73	45.7582	0.002	-0.066
73	45.7309	0.003	0.023	85	46.7422	0.003	-0.093
86	46.7809	0.003	-0.198	97	47.7248	0.002	-0.137
98	47.7639	0.004	-0.234	122	49.7790	0.002	-0.143
110	48.7647	0.002	-0.054	134	50.7633	0.002	-0.167
122	49.7477	0.005	-0.090	146	51.7677	0.001	0.054
134	50.7378	0.001	-0.040	158	52.7471	0.001	-0.029
146	51.7259	0.003	-0.014	170	53.7430	0.001	0.088
158	52.7190	0.001	0.073				
171	53.7819	0.001	0.009				

A least-squares linear fit to these data gives the following ephemeris for the maxima:

$$\text{HJD}_{\text{max}} = 2454346.79718(35) + 0.082165(6) \cdot (E - E_0) \quad (1)$$

and for the minima:

$$\text{HJD}_{\text{min}} = 2454346.83204(39) + 0.082187(6) \cdot (E - E_0) \quad (2)$$

where  $E_0 = 86$ .

Taking these two determination of period of modulation and the value obtained from ANOVA statistics, we conclude that mean value of period was 0.082159(6) days.

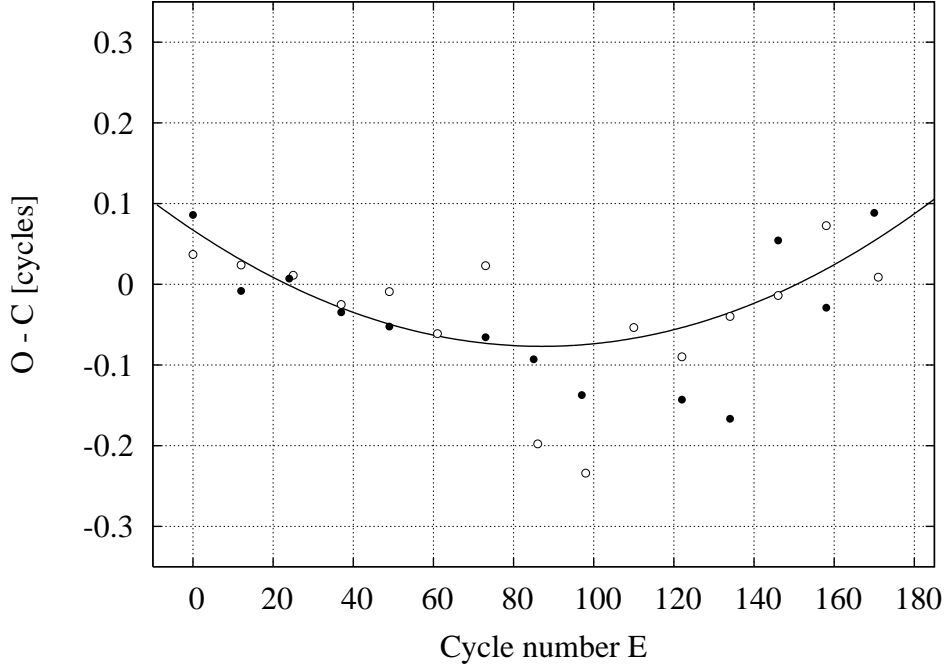


Figure 4:  $O - C$  diagram for the times of maxima (open circles) and minima (filled circles) observed in the light curve of BF Ara. Solid line is the fit to the combined  $O - C$  values assuming period derivative of  $\dot{P}/P_{sh} = -3.8(3) \times 10^{-5}$

The  $O - C$  values computed according to the ephemeris (1) and (2) are listed in Table 2 and also shown in Figure 4. It is clear that BF Ara, during our run, showed a clear change of period. A second-order polynomial fit the to moments of maxima is expressed by the following ephemeris:

$$\text{HJD}_{\text{max}} = 2454346.79271(68) + 0.082163(6) \cdot (E - E_0) + 1.10(14) \cdot 10^{-6} \cdot (E - E_0)^2 \quad (3)$$

and for the moments of minima:

$$\text{HJD}_{\text{min}} = 2454346.82347(74) + 0.082180(6) \cdot (E - E_0) + 2.10(16) \cdot 10^{-6} \cdot (E - E_0)^2 \quad (4)$$

To use the information both from maxima and minima, we used times and  $O - C$  values of minima, to construct virtual maxima. Then a second-order polynomial fit was made again resulting in quadratic term of value equal to  $1.56(11) \cdot 10^{-6}$ . This corresponds to the period derivative of  $\dot{P}/P_{sh} = -3.8(3) \times 10^{-5}$  which is with ideal agreement with value obtained in Sect. 4.1.

## 6 Discussion

### 6.1 The orbital period

First, we focus on modulation described in Sect. 4.2. Its peak-to-peak amplitude is 0.15 mag and one of several acceptable period values is 0.084176(21) days. The corresponding modulation appears stable during our 15-days run (see Fig. 5). We proceed to verify this period value whether it represents the orbital period of BF Ara.



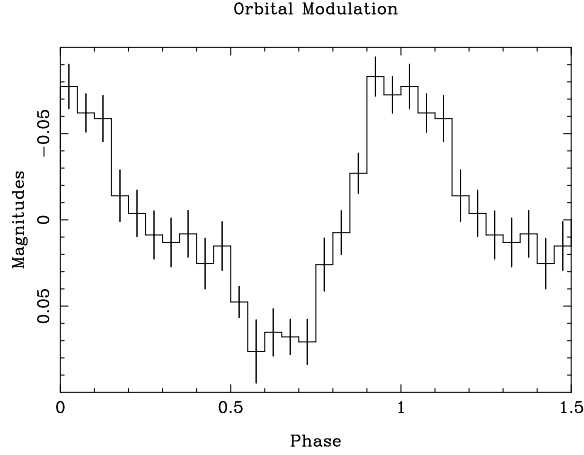


Figure 5: The mean shape of low amplitude modulation described in Sect. 4.2, after prewhitening with the light variations corresponding to the high amplitude permanent hump.

From their extensive observations of superhumps during superoutburst Kato et al. (2003) derived the superhump period  $P_{\text{sh}} = 0.08797(1)$ . It is known, that in SU UMa stars the superhump and orbital periods,  $P_{\text{sh}}$  and  $P_o$ , obey the Stolz and Schoembs (1984) relation. For this purpose one defines the superhump period excess as  $\epsilon = (P_{\text{sh}} - P_o)/P_o$ . In Fig. 6 we present a plot of superhump excess against the superhump period for all CVs with known orbital periods. For BF Ara we considered periods of several aliases for the secondary modulation of Sect 4.2 as tentative orbital periods and calculated the corresponding superhump excesses. All but one value obtained in this way deviated widely from the relation in Fig. 6. The only consistent value,  $\epsilon = 4.51\% \pm 0.03\%$  corresponds to our proposed orbital period of BF Ara and is plotted as filled square. It is clear that BF Ara follows this relation perfectly, giving credit to our belief that the secondary small amplitude modulation reflects the orbital wave. It is also worth to mention that its value of  $P_{\text{orb}} = 121.2$  minutes locates BF Ara in the period gap.

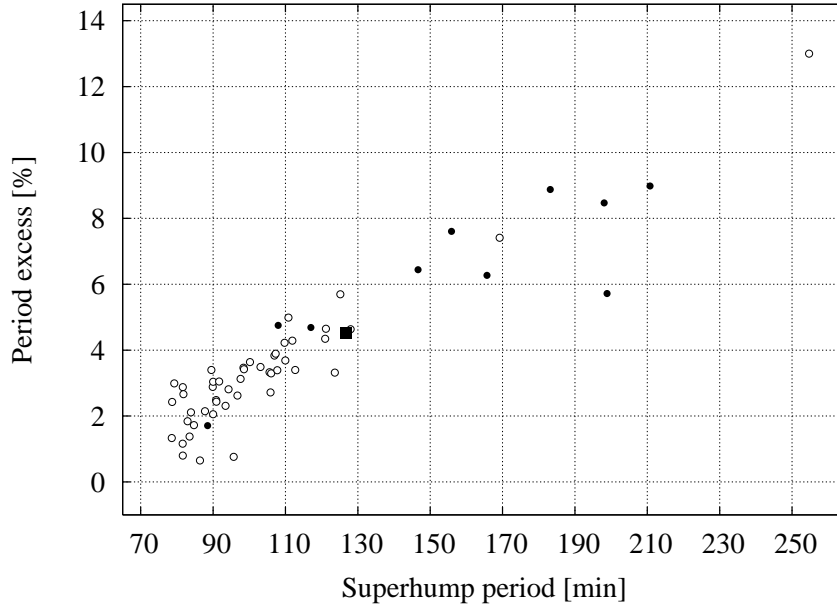


Figure 6: The relation between superhump period and period excess for ordinary SU UMa stars (open circles), objects other than dwarf novae (filled circles) and for BF Ara (filled square).

It has been established that the period excess in SU UMa stars correlates with the mass ratio  $q = M_2/M_1$ .

The corresponding relation may be approximated in the following way (Osaki 1985):

$$\varepsilon \approx \frac{0.23q}{1 + 0.27q} \quad (5)$$

Thus the known period excess  $\varepsilon$  of BF Ara can be used to estimate its mass ratio as  $q \approx 0.21$ .

Finally, we decided to give the ephemeris for maxima and minima of orbital modulation. They are as follows:

$$\text{HJD}_{\text{max}} = 2454345.8180(18) + P_{\text{orb}} \cdot N \quad (6)$$

$$\text{HJD}_{\text{min}} = 2454345.7886(18) + P_{\text{orb}} \cdot N \quad (7)$$

The moments of maxima and minima were determined by fitting data from Fig. 5 with a Fourier series up to  $2f_{\text{orb}}$  and then finding its extrema.

## 6.2 The negative superhumps

Now we verify whether the permanent hump modulation discussed in Sect. 4.1 fits the negative hump pattern. Its mean period was 0.082159(4) days, increasing at the rate of  $\dot{P}/P_h = 3.8(3) \cdot 10^{-5}$ . The mean amplitude of this modulation was 0.7 mag and its mean shape is shown in Fig. 7.

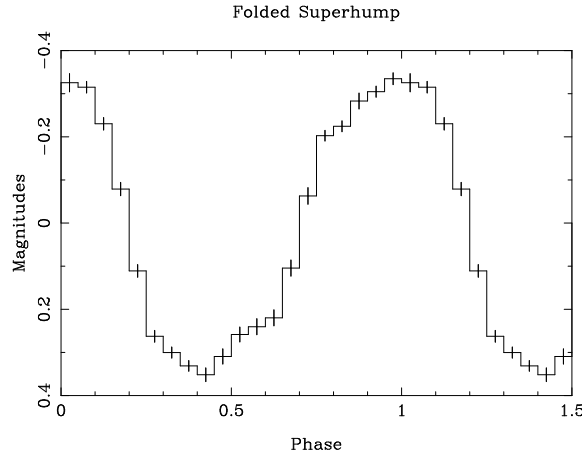


Figure 7: The mean shape of the negative superhump described in Sect. 4.1, after prewhitening with the light variations corresponding to the orbital hump.

There are cataclysmic variables exhibiting three close periods of modulation: the orbital wave, ordinary superhumps and, additionally, so called negative superhumps. The periods of ordinary and negative humps,  $P_{\text{sh}}$  and  $P_{\text{nh}}$  are respectively longer and shorter than the orbital period  $P_{\text{orb}}$ . It is believed that negative superhumps arise due to the classical precession of a tilted accretion disk. According to Wood and Burke (2007) in these stars the accretion disk is tilted out of the orbital plane. The negative hump modulation is caused by migration of the hot spot across the face of the disk. Without any tilt, the stream of accreted matter hits the edge of the disk roughly at the fixed distance from white dwarf in the orbital plane. For a tilted disc this situation happens only when the hot spot crosses the nodes of a disk. At other orbital phases stream misses outer parts of the disc, penetrating deeper in the gravitational potential well of the white dwarf. This in turn causes brightening of the

bright spot. Since only one face of the optically thick disk is visible, only one brightening per orbit is observed. A slow retrograde precession of the tilted disk results in a period slightly shorter than the orbital period.

Positive and negative superhumps are observed in variety of objects. Among them are double-degenerate systems such as AM CVn (Skillman et al. 1999), ordinary SU UMa stars like V503 Cyg (Harvey et al. 1995), classical novae like V1974 Cyg (Semeniuk et al. 1995, Retter, Leibowitz and Ofek 1997), X-ray systems containing neutron stars like V1405 Aql (Retter et al. 2002a) and intermediate polars like TV Col (Retter et al. 2002b). It is interesting that the super- and negative-hump periods in all objects seem to follow a unique relation. The respective period excess and defect are defined as  $\epsilon = (P_{sh} - P_{orb})/P_{orb}$  and  $\epsilon_- = (P_{nh} - P_{orb})/P_{orb}$ . In Fig. 8 taken from Retter et al. (2002a) we plot the defect and excess ratio  $\phi = \epsilon_-/\epsilon$  against the orbital period. The picture suggests a unique relation.

From the observed the hump and orbital periods we determine the period defect of BF Ara. It amounts to  $\epsilon_- = -2.44\% \pm 0.02\%$  and yields the ratio of the positive and negative hump defect and excess  $\phi = -0.540 \pm 0.006$ . We added the corresponding point in Fig. 8. It fits very well the overall trend, adding credit to our interpretation of this modulation as the negative hump.

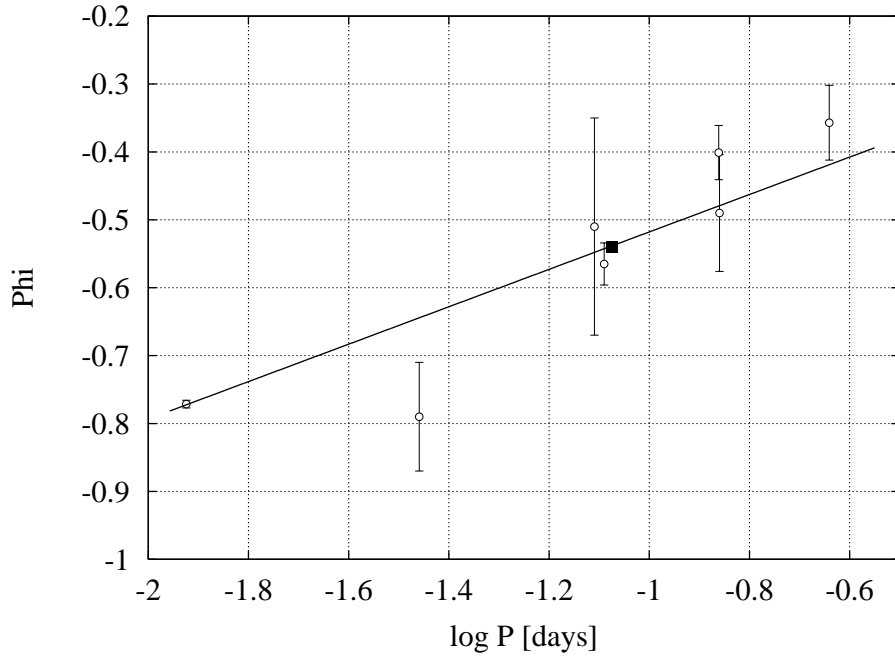


Figure 8: The relation between the ratio of negative and positive period excess and orbital period for cataclysmic variables showing both positive and negative superhumps. BF Ara is plotted with solid rectangle. Error of this determination is of the size of the symbol. Straight line corresponds to the fit given in equation (6).

Fitting a straight line to the points corresponding to individual variables one obtains the following relation:

$$\phi = 0.276(9) \cdot \log P - 0.232(14) \quad (8)$$

## 7 Summary

Our main conclusions may be summarized as follows:

- Light curve of BF Ara in quiescence is dominated by high amplitude signal with mean period of 0.082159(4) days which during two weeks observing run increased at the rate of  $\dot{P}/P_{sh} = 3.8(3) \cdot 10^{-5}$

- We interpret this periodicity as being due to a negative superhump. Such an interpretation is confirmed by the location of BF Ara in the Ritter et al. (2002a) relation,
- BF Ara seems to be a twin of V503 Cyg (Harvey et al., 1995) - both stars are very active (supercycles of 80–90 days), both show large amplitude negative superhumps in quiescence characterized by changing value period,
- Prewhitening of the original light curve with the main periodicity resulted in the discovery of another modulation with constant period equal to 0.084176(21) days, which is interpreted as the orbital period of the system. This value makes BF Ara another in-the-gap cataclysmic variable,
- Knowing the ordinary superhump period measured by Kato et al. (2003) we were able to calculate the period excess as equal to  $4.51\% \pm 0.03\%$  which indicates the mass ratio of  $q \approx 0.21$ .

**Acknowledgments.** We acknowledge generous allocation of the SAAO 1-m telescope time. We would like to thank Prof. Józef Smak for fruitful discussions. This work was supported for SALT grant number 76/E-60/SPB/MSN/P-03/DWM 35/2005-2007.

## References

- [1] Bruch, A., 1983, *IBVS No.* 2286
- [2] Harvey, D.A., Skillman, D.R., Patterson, J., Ringwald, F.A., 1995, *PASP*, 107, 551
- [3] Kato, T., Kunjaya, C., 1995, *PASJ*, 47, 163
- [4] Kato, T., Stubbings R., Pearce, A., Nelson, P., Monard, B., 2001, *IBVS No.* 5119
- [5] Kato, T., Bolt, G., Nelson, P., Monard, B., Stubbings, R., Pearce, A., Yamaoka, H., Richards, T., 2003, *MNRAS*, 341, 901
- [6] Olech, A., Mularczyk, K., Kedzierski, P., Zloczewski, K., Wisniewski, M., Szaruga, K., 2006, *Astron. Astrophys.*, 452, 933
- [7] Osaki, Y., 1985, *Astron. Astrophys.*, 144, 369
- [8] Osaki, Y., 1995, *PASJ*, 47, 25
- [9] Osaki, Y., 1996, *PASP*, 108, 39
- [10] Pattreson, J., Masi, G., Richmond, M.W. et al., 2002, *PASP*, 114, 721
- [11] Retter, A., Leibowitz, E.M., Ofek, E.O., 1997, *MNRAS*, 286, 745
- [12] Retter, A., Chou, Y., Bedding, T.R., Naylor, T., 2002a, *MNRAS*, 330, L37
- [13] Retter, A., Hellier, C., Augusteijn, T., Naylor, T., Bedding, T.R., Bembrick, C., McCormick, J., Velthuis, F., 2002b, *MNARS*, 340, 679
- [14] Robertson, J.W., Honeycutt, R.K., Turner, G.W., 1995, *PASP*, 107, 443
- [15] Rutkowski, A., Olech, A., Mularczyk, K., Boyd, D., Koff, R., Wisniewski, M., 2007, *Acta Astron.*, 57, 267

- [16] Schapley, H., Swope, H.H., 1934, *Harvard Annals*, 80, No. 5
- [17] Schwarzenberg-Czerny, A., 1991, *MNRAS*, 253, 198
- [18] Schwarzenberg-Czerny, A., 1996, *ApJ Letters*, 460, L107
- [19] Semeniuk, I., de Young, J.A., Pych, W., Olech, A., Ruszkowski, M., Schmidt, R.E., 1995, *Acta Astron.*, 45, 365
- [20] Skillman, D.R., Patterson, J., 1993, *ApJ*, 417, 298
- [21] Skillman, D.R., Patterson, J., Kemp, J., Harvey, D.A., Fried, R., Retter, A., Lipkin, Y., Vanmunster, T., 1999, *PASP*, 111, 1281
- [22] Stetson, P.B., 1987, *PASP*, 99, 191
- [23] Stolz, B., Schoembs, R., 1984, *Astron. Astrophys.*, 132, 187
- [24] Warner, B., 1995, *Cataclysmic Variable Stars*, Cambridge University Press.
- [25] Wood, M.A., Burke, C.J., 2007, *ApJ*, 661, 1042